IL NUOVO CIMENTO **45 C** (2022) 101
DOI 10.1393/ncc/i2022-22101-1

COMMUNICATIONS: SIF Congress 2021

# Reconstruction and trigger performance studies of the New Small Wheel of the ATLAS detector

V. D'AMICO([1])([2]) on behalf of the ATLAS MUON COLLABORATION

([1]) *INFN, Sezione di Roma Tre - Roma, Italy*
([2]) *Dipartimento di Matematica e Fisica, Università degli Studi Roma Tre - Roma, Italy*

received 29 January 2022

**Summary.** — The expected instantaneous luminosity increase for Run 3 and the high luminosity phase of LHC up to $7.5 \times 10^{34}$ fb$^{-1}$ requires upgrading the muon spectrometer of the ATLAS experiment. The New Small Wheel (NSW) consist of new generation gas detectors, Micromegas and small-strip Thin Gap Chambers, replacing the first measuring station in the forward region of the muon spectrometer. This contribution presents the muon trigger and reconstruction performance of the NSW. These performances are studied through Monte Carlo simulations with different detector configurations and background levels, and compared with data acquired with particle beams and cosmic muons.

## 1. – The New Small Wheel upgrade

The instantaneous luminosity provided by the Large Hadron Collider (LHC) during the Run3 and the High Luminosity LHC (HL-LHC) phase is planned to increase up to $7.5 \times 10^{34}\,\mathrm{s}^{-1}\mathrm{cm}^{-2}$. A huge increase of particle rates is expected, mainly in the high-rapidity regions of the ATLAS experiment [1]. This would result in a loss in efficiency of the muon detectors of the first end-cap station of the muon spectrometer. The larger amount of particles would affect the trigger and tracking performances, introducing the triggering of many fake non-prompt muons and increasing the background rates. The trigger rate would exceed the readout bandwidth dedicated to the ATLAS L1 muon trigger and the thresholds should be increased, losing muons with low transverse momentum ($p_{\mathrm{T}}$). For these reasons, an upgrade of the muon spectrometer has been designed to cope with the expected flux of particles in the forward regions, in the pseudorapidity ($\eta$) range $1.3 < |\eta| < 2.7$, maintaining the design performances for the entire Run3 and HL-LHC: the New Small Wheel [2]. Two new detector technologies, Micromegas (MM) [3] and small-strip Thin Gap Chambers (sTGC) [4], are exploited to provide excellent tracking and trigger performances in this new demanding conditions. The main requirements are substantially reducing the fakes trigger rate at L1, reconstructing the online muon

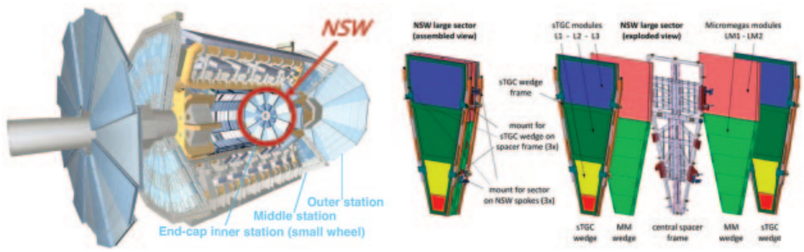


Fig. 1. – Schematic diagram of the NSW inside the ATLAS detector, showing the structure of a sector of the NSW and the position of MM and sTGC chambers.

tracks with 95% efficiency, and providing excellent spatial and angular resolutions: less than 50 $\mu$m for the reconstructed segments in the wheel, and less than 1 mrad for on-line matching with the Big Wheel. Each wheel is made of 16 sectors and each sector is composed of two sTGC wedges and two MM wedges, as shown in fig. 1.

The sTGC wedges are made of 3 quadruplet modules, each composed of four layers. The MM wedges are, instead, made of two quadruplet modules, made by 2 precision and 2 stereo strip layers, with the readout strips tilted by $+/-1.5°$, providing second coordinate information. The quadruplet assembly of the two detectors is performed in different construction sites, while NSW sectors are assembled at CERN, as described in fig. 1, forming a sector with eight sTGC and eight MM detector layers.

MM detectors, schematically described in fig. 2, consist in 5 mm drift gap separated from an amplification gap of 128 $\mu$m by a very thin metallic mesh, having a wire diameter of 30 $\mu$m with an opening of 70 $\mu$m. The metallic mesh is floating over pillars of insulating material placed on the anode readout and is transparent to electrons, providing also a fast evacuation of the positive ions.

Both regions are filled with a gas mixture of Ar:$CO_2$ (93%:7%). The readout layer is made of resistive strips of 300 $\mu$m width with a pitch of 450 $\mu$m capacitively coupled with readout Cu strips placed below them. The resistivity of $>0.5\,\mathrm{M}\Omega/\square$ (per square) of the resistive strips protects the detector from the sparks that may occur in the amplification gap. This detector is primarily used for tracking, having a spatial resolution $\sim$100 $\mu$m for small angles and 72 $\mu$m for perpendicular tracks, as seen from test beam data on final modules. The sTGC are multiwire ionization chambers operated in quasi-saturated mode. Each layer is made of two cathodes with anode wires in the gap between them, as visible from fig. 2. One cathode is divided into large pads used for the trigger, while

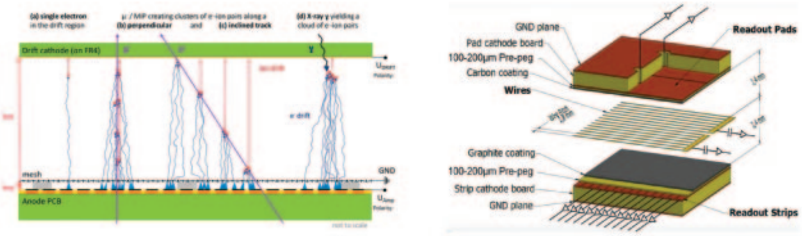


Fig. 2. – Sketch of the layout cross-section and operating principle of a MM detector (left), and picture of the layout of an sTGC detector (right).

the other cathode is made of strips with a 3.2 mm pitch, providing precision track reconstruction in the $\eta$ direction. Wires have a 1.5 mm pitch in the direction orthogonal to the strips and (readout in groups of 8 wires) will provide second coordinate position information. The sTGC are operated at a voltage of 2.9 kV with a 55:45 gas mixture of $CO_2$ and n-pentane, providing 95% reconstruction efficiency and 75 $\mu$m position resolution for perpendicular tracks.

## 2. – Simulation of the New Small Wheel

Monte Carlo (MC) simulated muon samples are used to study the tracking and trigger performances of the NSW. The NSW geometry is simulated starting from the nominal design, and taking into account all the support materials, shielding, cables and frames. The so called "as built" parameters are used to correct the geometry for the deviations in the construction from the nominal design. Gas volumes inside the gaps, and the readout channels, which are over one million for MM and about 320 thousands for sTGC, are also faithfully simulated. The alignment system allows following any deformation during operation. Also operational conditions different from nominal can be simulated, such as dead channels, layer's amplification voltage (HV), etc. The simulation of the incident particle interaction with the detectors is performed using the ATLAS version of the GEANT4 toolkit. This interaction results in hits, which are then digitized to simulate the response of the detector and the readout electronics, giving in output a number of firing strips each with a collected charge and timing information. The tracking and trigger algorithm exploits this digitized information of the several detector's layers to reconstruct tracks and to select muon candidates. Strip clusters are built grouping neighbouring firing strips having a strip charge above the threshold, and the position of the cluster is then reconstructed. The standard method is the charge centroid, that consists in a weighted position using the cluster's strip charge as weights. For the MM, a second method is available, the micro-Time Projection Chamber ($\mu$TPC), which exploits the time information and the drift velocity of the electrons to better reconstruct the position at larger angles, where the charge is spread in a larger number of strips, as visible from fig. 3. Also the sTGC cluster position reconstruction method is being optimised.

Track reconstruction performances evaluated with cosmic rays are reproduced in the simulation. Track reconstruction efficiency is dependent on the HV applied to the detector, and in the simulation it is possible to map the reconstruction efficiency of the clusters in each NSW sector following the real HV working points. High voltage change is implemented in digitization scaling the amplification following the dependence of the

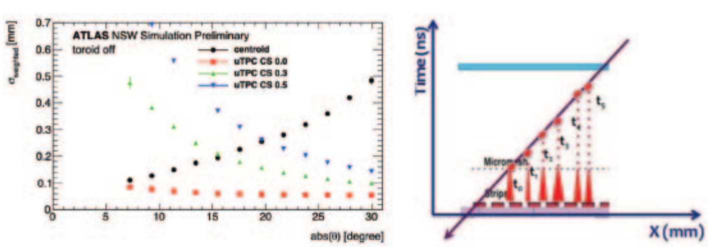


Fig. 3. – Resolution of the MM eta layers for different clusterization methods evaluated from MC samples with different charge sharing (CS) values (left) [5]. Graphical picture of the $\mu$TPC clusterization method (right).

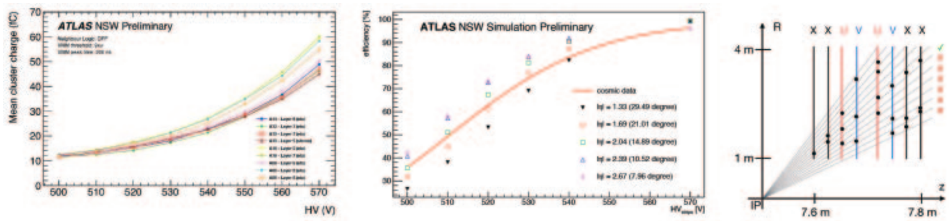


Fig. 4. – Mean Micromegas cluster charge (left), and cluster reconstruction efficiency (center) as a function of the amplification voltage. The clusters were reconstructed using the centroid. The data points come from simulation, and the curve is obtained from the cosmic ray data, integrating over all the reconstructed angles [5]. Schematic view of the trigger roads in the $Rz$ plane for the MM trigger (right).

charge of cluster from the voltage measured with cosmic rays, as visible in fig. 4. Trigger algorithms are also simulated to evaluate their expected performances and tune the coincidence logic. MM and sTGC have two stand-alone trigger algorithms. The sTGC trigger works using pads and selects a trigger candidate if there are 3 out of 4 aligned firing pads for each of the two quadruplets.

MM trigger exploits strip information, building roads for each detector layer in range of slopes in the $Rz$ plane, pointing to the interaction point, as visible from fig. 4. The intersection of roads of the three types, eta (X), and the two stereo (U and V), if satisfying the requirement of the coincidence logic of $2X + 1U + 1V$ in a 4 bunch crossing window, makes it a trigger candidate. Performance studies on efficiencies and trigger rates are being performed using minimum bias and pile-up MC samples to simulate the background expected during Run 3 and HL-LHC, coming from multiple interactions and "cavern" background of particles with long life time from previous interactions.

## 3. – Conclusions

The two NSWs are installed in the experiment and will be ready for the start of the Run 3 data taking. The NSW simulation is fundamental for optimizing the trigger and tracking algorithms, and the experimental conditions are reproducible in the simulation in order to evaluate the real performances. Track reconstruction performance is consistent with those measured with cosmic rays and particle beams, while a trigger performance study is ongoing using simulations of the cavern background expected in the next Runs.

REFERENCES

[1] ATLAS Collaboration, *JINST*, **3** (2008) S08003.
[2] ATLAS Collaboration, *New Small Wheel Technical Design Report*, CERN-LHCC-2013-006.
[3] Alexopoulos T. *et al.*, *Nucl. Instrum. Methods A*, **955** (2020) 162086.
[4] Smakhtin V. *et al.*, *Nucl. Instrum. Methods A*, **598** (2009) 196.
[5] ATLAS Collaboration, *New Small Wheel Public Results*, ATLAS public repository, `https://twiki.cern.ch/twiki/bin/view/AtlasPublic/NSWPublicResults`.